Cerebral Cortex, February 2019;29: 852–862

doi: 10.1093/cercor/bhy287
Advance Access Publication Date: 14 November 2018
Original Article

ORIGINAL ARTICLE

Person-Based Brain Morphometric Similarity is Heritable and Correlates With Biological Features

Gaelle E. Doucet[1], Dominik A. Moser[1], Amanda Rodrigue[2], Danielle S. Bassett [3,4,5,6], David C. Glahn[2,7] and Sophia Frangou[1]

[1]Department of Psychiatry, Icahn School of Medicine at Mount Sinai, New York, NY 10029, USA, [2]Department of Psychiatry, Yale University School of Medicine, New Haven, CT 06510, USA, [3]Department of Bioengineering, University of Pennsylvania, Philadelphia, PA 19104, USA, [4]Department of Electrical & Systems Engineering, University of Pennsylvania, Philadelphia, PA 19104, USA, [5]Department of Physics & Astronomy, University of Pennsylvania, Philadelphia, PA 19104, USA, [6]Department of Neurology, University of Pennsylvania, Philadelphia, PA 19104, USA and [7]Olin Neuropsychiatric Institute, Institute of Living, Hartford Hospital, Hartford, CT 06106, USA

Address correspondence to Sophia Frangou and Gaelle E. Doucet. Department of Psychiatry, Icahn School of Medicine at Mount Sinai, 1425 Madison Avenue, New York, NY 10029, USA. Email: sophia.frangou@mssm.edu (S.F.)/gaelle.doucet@mssm.edu (G.E.D.)

Abstract

The characterization of the functional significance of interindividual variation in brain morphometry is a core aim of cognitive neuroscience. Prior research has focused on interindividual variation at the level of regional brain measures thus overlooking the fact that each individual brain is a person-specific ensemble of interdependent regions. To expand this line of inquiry we introduce the person-based similarity index (PBSI) for brain morphometry. The conceptual unit of the PBSI is the individual person's brain structural profile which considers all relevant morphometric measures as features of a single vector. In 2 independent cohorts (total of 1756 healthy participants), we demonstrate the foundational validity of this approach by affirming that the PBSI scores for subcortical volume and cortical thickness in healthy individuals differ between men and women, are heritable, and robust to variation in neuroimaging parameters, sample composition, and regional brain morphometry. Moreover, the PBSI scores correlate with age, body mass index, and fluid intelligence. Collectively, these results suggest that the person-based measures of brain morphometry are biologically and functionally meaningful and have the potential to advance the study of human variation in multivariate brain imaging phenotypes in healthy and clinical populations.

Key words: age, brain morphometry, fluid intelligence, heritability, intersubject variability

Introduction

A core aim of cognitive neuroscience is to identify the functional significance of interindividual variation in brain organization in healthy and in clinical populations. Here, we focus specifically on brain morphometry as assessed using magnetic resonance imaging (MRI) as this is the most widely used neuroimaging method in research and clinical settings. The investigation of interindividual variation in brain morphometry has adopted 2 main analytical methods, variable-based and person-based. Variable-based approaches aim to identify similarities between

simple or composite structural MRI features across individuals (Song et al. 2013; Holmes et al. 2016; Seidlitz et al. 2018). Such analyses have been instrumental in establishing links between brain morphometric variation and age, sex, and cognition (Hulshoff Pol et al. 2006; Deary et al. 2010; Kanai and Rees 2011; Ruigrok et al. 2014) but have been criticized for fostering the incorrect impression that the findings can be generalized to every individual person (von Eye and Bogat 2006). Person-based analyses aim to identify subgroups of individuals with multiple similar brain morphometric features using a variety of clustering algorithms. This approach has been most commonly used to identify clusters of individuals at risk of adverse clinical outcomes (Koutsouleris et al. 2009; Rocha-Rego et al. 2014; Rathore et al. 2017) but remain largely uninformative at the level of an individual person. The degree of homogeneity is defined at the level of clusters but not individuals; in fact, the same individual may be assigned to different clusters depending on the algorithm (Gelbard et al. 2007). Therefore, the field is lacking a measure that can be informative at the level of each individual person.

In this context, we propose the "person-based similarity index" (PBSI) as a novel metric of similarity between the brain structural profile of an individual study participant and that of all other participants. We constructed a PBSI for subcortical volume (PBSI-SVol) and another for cortical thickness (PBSI-CThi) as subcortical and cortical brain regions have partially distinct genetic, developmental and environmental correlates (Miller et al. 2016; Wen et al. 2016). Cortical morphometry can be described in terms of thickness and surface area. These 2 measures are thought to reflect different biological processes; cortical thickness has been linked to dendritic arborization and pruning (Huttenlocher 1990) while surface area has been associated with cortical gyrification (Lewitus et al. 2013). Consequently, cortical thickness and surface area have distinct genetic correlates (Panizzon et al. 2009) and developmental trajectories (Raznahan et al. 2011; Wierenga et al. 2014). Here we focus specifically on cortical thickness because of the prodigious evidence linking cortical thickness to cognition in healthy populations (Narr et al. 2007; Fjell et al. 2010; Karama et al. 2011) and in neuropsychiatric disorders (Thompson et al. 2007; Boedhoe et al. 2018; Hibar et al. 2018; Van Erp et al. 2018; van Rooij et al. 2018; Whelan et al. 2018).

The process of computing the PBSI begins by calculating the interindividual correlation coefficient for each pair of individual-specific imaging profiles yielding $n-1$ coefficients per individual (where n is the group size) (Fig. 1*a*,*b*). These correlations quantify the similarity of the imaging profile of each individual to that of each of the other group members (Fig. 1*b*). Averaging these correlation coefficients across all group members yields a PBSI score, which provides a quantitative characterization of the similarity of the participants' imaging profiles (Fig. 1*c*). High values indicate that the imaging profile of any one group member accurately predicts the profiles of all other members, whereas low values signify low consistency among the imaging profiles of the group members. The subcortical volume and cortical thickness profiles were constructed as 2 separate vectors by respectively concatenating measures of subcortical volume and cortical thickness. To ascertain the foundational validity of the PBSI scores we tested 3 predictions: 1) that the PBSI scores would be replicable and robust to variation in data acquisition and analyses parameters and to sample composition; 2) that the PBSI scores would be independent to variation in discrete brain regional measures; and 3) that the PBSI would show evidence of heritability as inferred from prior evidence that brain morphometry is influenced by genetic

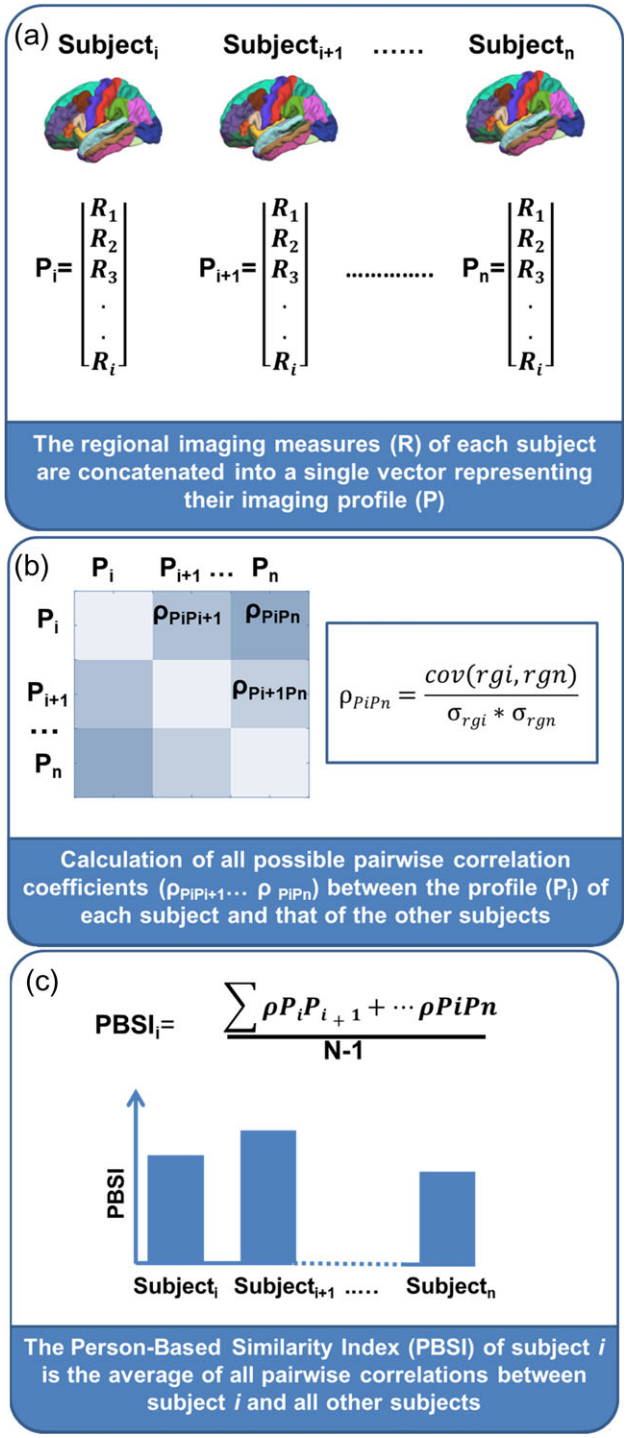

Figure 1. Pipeline for computing a person-based similarity index. (*a*) Creation of a structural profile (P) using regional measures (R) (e.g., cortical thickness or subcortical volumes) for each subject *i*. (*b*) Computation of Spearman's correlation between each pair of individual profiles. The *n* profiles (P) are first converted to ranks (ρg_i,… ρg_n), cov(ρg_i,ρg_n): covariance of the rank variables (ρg_i and ρg_n), σ: standard deviation of the rank variables. (*c*) For subject *i*, the person-based similarity index (PBSI) is computed as the average of all pairwise correlations between the subject *i* and all other subjects.

factors (Blokland et al. 2012; McKay et al. 2014; Strike et al. 2018). To test these predictions, we computed multiple reliability analyses on 2 independent cohorts of healthy individuals from

the Human Connectome Project (HCP) (Van Essen et al. 2013) and the Cambridge Center for Ageing and Neuroscience study (CamCAN) (Shafto et al. 2014; Taylor et al. 2017). We further predicted that the PBSI will 1) differ between men and women since sex is a major contributor to brain structural variation (Wierenga et al. 2017; Ritchie et al. 2018); 2) be inversely associated with age (Hedman et al. 2012; Miller et al. 2016) and body mass index (BMI), a surrogate but informative marker of cardiometabolic health, as both of these features are known to increase brain structural variation (Miller et al. 2016); and 3) be positively associated with measures of general intelligence in line with recent reports linking intelligence to similarity in brain anatomical networks (Seidlitz et al. 2018).

Materials and Methods

Samples

We used data from 1756 healthy adults derived from the Human Connectome Project (www.humanconnectome.org) (Van Essen et al. 2013) and the CamCAN repository (www.mrc-cbu.cam.ac.uk/datasets/camcan) (Shafto et al. 2014; Taylor et al. 2017). The most recent release of HCP database comprised 1113 individuals (606 women), aged 22–37 years (mean [standard deviation {std}] = 28.80 [3.70] years). The CamCAN sample comprised 643 individuals (328 women), aged 18–88 years (mean [std] = 54.07 [18.54] years).

Neuroimaging Data Acquisition

In the HCP sample, the structural MRI (sMRI) data were acquired on a 3 T Siemens Connectome-Skyra scanner using a T1-weighted (T1w), 3D magnetization-prepared rapid gradient-echo (MPRAGE) sequence with the following parameters: repetition time (TR)/time to echo (TE)/inversion time (TI) = 2400/2.14/1000 ms, voxel size = 0.7 mm isotropic, flip angle = 8°, field of view (FOV) = 224 × 224 mm^2, duration of acquisition: 7 min 40 s.

In the CamCAN sample, the sMRI data were acquired on a 3 T Siemens TIM Trio scanner with a 32-channel head coil, using a T1-weighted, 3D MPRAGE sequence with the following parameters: TR/TE/TI = 2250/2.99/900 ms, voxel size = 1 mm isotropic, flip angle = 9°, FOV = 256 × 240 × 192 mm^3, duration of acquisition: 4 min 32 s.

sMRI Data Processing and Quality Control

Parcellation and segmentation of the sMRI datasets of the HCP and CamCAN participants was implemented in FreeSurfer (http://surfer.nmr.mgh.harvard.edu/). For the HCP sample, we downloaded FreeSurfer 5.3.0 outputs that had been processed and quality controlled using the latest HCP protocols (https://www.humanconnectome.org/storage/app/media/documentation/s1200/HCP_S1200_Release_Appendix_IV.pdf). For the CamCAN sample, we analyzed T1w images using FreeSurfer 6.0. The steps included removal of nonbrain tissue using a hybrid watershed/surface deformation procedure (Segonne et al. 2004), automated Talairach transformation, segmentation of the subcortical white matter, and deep gray matter volumetric structures (Fischl et al. 2002, 2004) intensity normalization (Sled et al. 1998), tessellation of the boundary between the gray and white matter, automated topology correction (Fischl et al. 2001; Segonne et al. 2007), and surface deformation following intensity gradients to optimally place the gray/white matter boundaries and gray/cerebrospinal fluid borders at the location where the greatest shift in intensity defines the transition to the other tissue class. All participants' data passed the quality control protocols developed by the ENIGMA initiative (http://enigma.ini.usc.edu/).

Extraction of Subcortical Volume and Cortical Thickness Measures

Following FreeSurfer segmentation and parcellation based on the Desikan atlas (Desikan et al. 2006), we obtained 64 cortical thickness measures and 16 subcortical volume measures (Supplemental Table S1) for each HCP and CamCAN study participant. Prior to being entered into further analyses, subcortical volumes in the HCP and CamCAN samples were adjusted for variation in intracranial volume (ICV) in each sample in accordance to standard protocols (Pintzka et al. 2015) using the following equation: $Vol_{adj} = Vol - \beta * (ICV - \overline{ICV})$, where, Vol_{adj} is the ICV-adjusted volume, Vol is the original uncorrected volume, β is the slope from the linear regression of Vol on ICV, ICV is the ICV of a study participant and $\overline{ICV}$ is the mean ICV across all participants in each study sample.

Computation of the PBSI Scores

Separately in the HCP and CamCAN samples, we computed a PBSI score for subcortical volume (PBSI-SVol) and another for cortical thickness (PBSI-CThi), using an identical 3-step procedure (Fig. 1). First, we created the subcortical volume and cortical thickness profile of each participant by concatenating the corresponding Freesurfer derived morphometric measures detailed in Supplemental Table S1 (Fig. 1*a*). Second, we calculated the interindividual Spearman's correlation coefficient between the subcortical volume or cortical thickness profile of any given participant with the corresponding profiles of each of all the other sample participants (Fig. 1*b*). Third, the $n-1$ interindividual correlation coefficients (n refers to the total number of participants in each sample) for subcortical volume and cortical thickness were averaged separately to yield one corresponding PBSI score per participant (Fig. 1c). Higher scores (with a maximum of 1) denote greater similarity between the subcortical volumes or cortical thickness profiles of an individual participant with those of the other participants in the same sample. Outliers were defined as those having PBSI scores more than 4 standard deviations from the sample mean; this resulted in the removal of 5 participants in the HCP (mean [std] age: 27.6 (3.4), 3 females) and 7 participants in the CamCAN sample (mean [std] age: 71.9 [22.3], 1 female).

The matlab function used to compute the PBSI score is available at: https://www.mathworks.com/matlabcentral/fileexchange/69 158-similarityscore.

Contribution of Regional Brain Measures to the PBSI

The contribution of the regional brain measures on the PBSI scores was investigated using 2 approaches. The first one was a bootstrap resampling approach. For the PBSI-CThi, we created cortical thickness profiles by randomly grouping variables in increments of 10 (i.e., from 10 to 60 regions selected) and we then recalculated the PBSI for each individual, 100 times. For the PBSI-SVol, we created profiles by randomly grouping half of the variables (i.e., 8) and recalculated the PBSI for each individual, 100 times. The second analysis was a leave-one-out approach that allowed us to quantify the contribution of each regional brain measure to the PBSI scores. For the leave-one-out analyses, the PBSI-SVol and PBSI-CThi scores of each

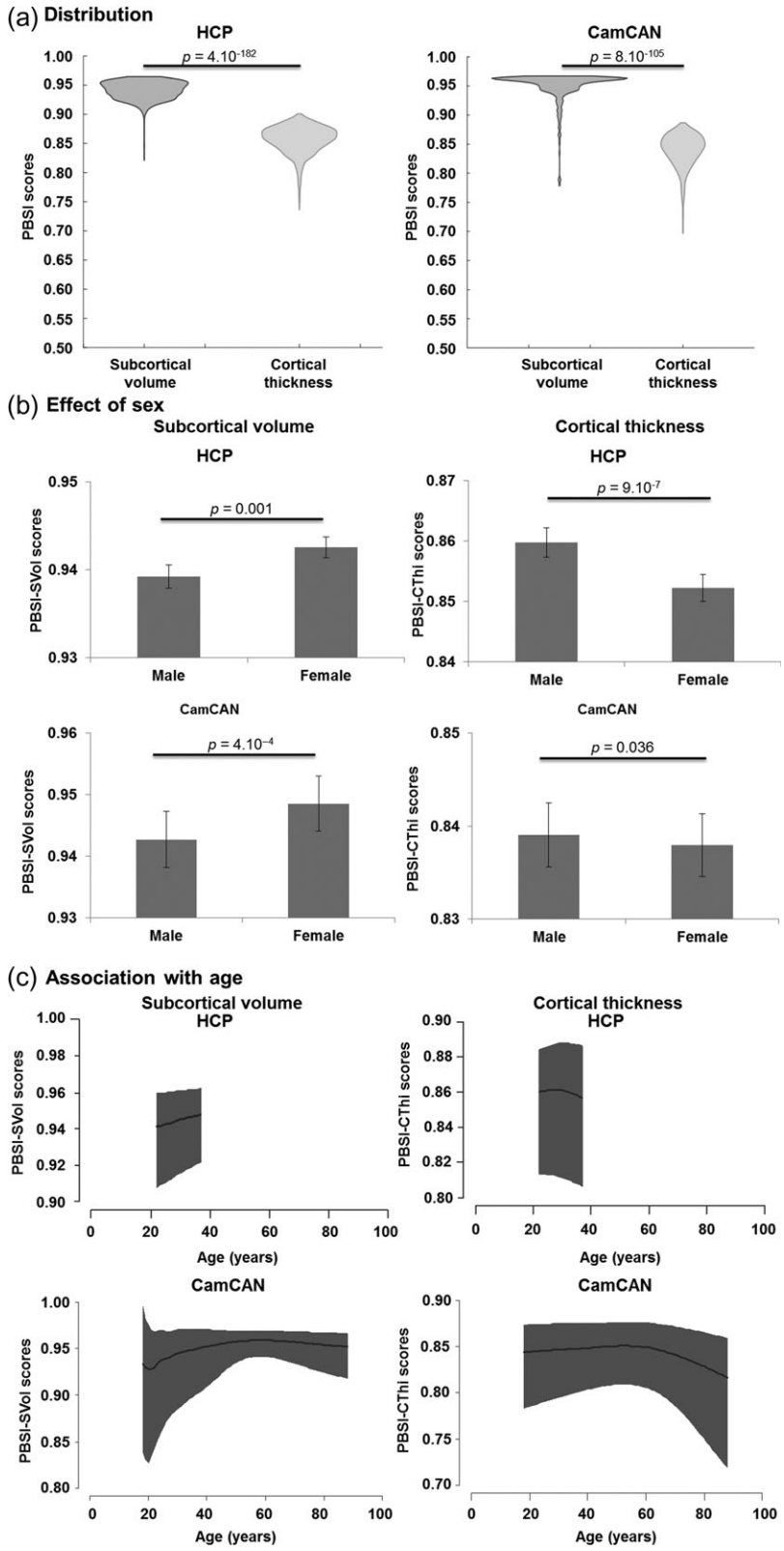

Figure 2. Person-based similarity index for subcortical volume and cortical thickness in the HCP and CamCAN Samples. (*a*) Violin plots of the person-based similarity index (PBSI) scores for subcortical volume and cortical thickness in the Human Connectome Project (HCP) and the Cambridge Center for Ageing and Neuroscience (CamCAN) samples. *P*-values are based on Wilcoxon Tests. (*b*) Sex differences in PBSI scores in the HCP and CamCAN samples. Barplots depict the mean and 95% confidence interval (CI) for men and women. *P*-values are based on Mann–Whitney *U* tests. (c) Association between age and PBSI scores in the HCP and CamCAN sample. Dark areas represent 95% CI.

participant were recalculated after leaving out one regional brain measure at a time (Supplemental Table S4). The regional contributions to the PBSI-CThi in early, middle, and late adulthood in the CamCAN sample are visualized in Supplemental Figure S1.

Association Between PBSI Scores With Age and Sex

Sex differences in the PBSI-SVol and PBSI-CThi were assessed separately in the HCP and CamCAN samples using Mann–Whitney *U* tests. We employed curve estimation regression to determine the association between PBSI scores and age. We used Spearman's correlation analyses to examine the association between age and PBSI scores in 3 age brackets reflecting early adulthood (age range: 18–39 years), middle adulthood (age range: 40–59 years) and late adulthood (age range: 60–88 years). Further we recomputed the PBSI scores within each age bracket and compared them using Kruskal–Wallis tests. Both the HCP and CamCAN samples contributed data to the early adulthood age bracket while the 2 other age brackets included data from the CamCAN sample only.

Heritability of the PBSI Score

Heritability estimates were calculated in the HCP sample only, in which the relevant data were available, using Sequential Oligogenic Linkage Analysis Routines (SOLAR) software (Almasy and Blangero 1998). Heritability estimates range from 0 to 1 and indicate the degree of phenotypic variation is due to genetic factors. Heritability was estimated by partitioning the phenotypic covariance matrix into genetic and environmental components as $h^2 = \sigma^2_G/(\sigma^2_G + \sigma^2_E)$, where σ^2_G represents additive genetic variance and s^2_E represents random environmental effects. The covariance matrix, or Ω, is composed of an $n \times n$ kinship matrix (R) and a $n \times n$ identity matrix (I) as follows: $\Omega = R\sigma^2_G + I\sigma^2_E$. The PBSI scores were standardized and then normalized using an inverse Gaussian transform before being entered into the heritability analysis. The normal distribution of the data is a requirement for the SOLAR software in order to compute an accurate heritability score (see Lynch and Walsh 1998; Blangero et al. 2013). The choice of applying an inverse normalization transform over other options, is based on the fact that this transform retains most of the original information, and yet provide a new normally distributed dataset. The rationale for this approach can be found at: https://brainder.org/2011/07/13/inverse-normal-transformation-in-solar/. Age, age^2, sex, and their interactions (age × sex, age^2 × sex) were tested as covariates of interest by comparing the likelihood of a model estimating the covariate effect to the likelihood of a model where the covariate effect was constrained to zero.

Association Between PBSI Scores and Intelligence

Effects of age (in the HCP sample), age^2 (in the CamCAN sample), and sex (both samples) were regressed out of the PBSI scores prior to estimating their association with the fluid and crystallized intelligence (defined in "nonimaging variables" section of the Supplemental Table S1). Crystallized intelligence is thought to represent knowledge and skills acquired through learning (Horn and Cattell 1966). By contrast, fluid intelligence is thought to reflect acquisition of new associations and novel, adaptive problem solving (Horn and Cattell 1966). In the HCP dataset, measures of crystallized and fluid intelligence were derived from cognitive tests in the NIH Toolbox-Cognition Battery (www.nihtoolbox.org) using previously published reliable and reproducible procedures (Akshoomoff et al. 2013; Heaton et al. 2014). In the CamCAN sample, fluid intelligence was measured with the Cattell Culture Fair Intelligence Test (Cattell 1971) using established published protocols (Kievit et al. 2016). We assessed these associations using both linear (Spearman's correlation) and nonlinear (curve estimation regression–quadratic association) methods.

Association Between PBSI Scores and Body Mass Index

In the HCP sample, we examined the association between BMI and PBSI scores using both linear (Spearman's correlation) and nonlinear (curve estimation regression–quadratic association) methods, in men and women separately.

Reliability Analyses

We examined the stability of the PBSI scores after adjusting the cortical thickness measures for the average cortical thickness and the subcortical volume measures for the average subcortical volume (instead of ICV). Results are reported in the supplementary material. Parcellation schemes are known to affect results (Arslan et al. 2018). Therefore, we extracted 148 cortical thickness measures based on the Destrieux atlas (Fischl et al. 2004) (https://surfer.nmr.mgh.harvard.edu/fswiki/CorticalParcellation). We recalculated PBSI-CThi scores and repeated all the analyses. We also assessed test–retest reliability in the 45 HCP participants who had 2 scans with an average interval between scans of 139.3 (std: 68.2) days. We computed the PBSI-SVol and PBSI-CThi scores for each scan and calculated their intraclass correlation coefficient (ICC). Lastly, we examined the stability of the PBSI scores as a function of sample size. To this purpose, we applied a bootstrap approach by randomly resampling 10–90% from the original sample (in 10% increments) 1000 times. We then recomputed the PBSI scores on each bootstrapped subset, for subcortical volume and cortical thickness separately.

Results

The PBSI Across Samples

Both PBSI scores showed a replicable pattern of range and distribution in the HCP and CamCAN samples. Higher PBSI scores denote greater similarity in subcortical and cortical profiles, the maximum possible score for each PBSI score is 1 which denotes the greatest possible similarity between an individual participant and all other participants in the same sample. Figure 2*A* depicts the distribution of the PBSI-SVol and PBSI-CThi scores in the HCP and CamCAN samples. In both HCP and CamCAN samples, PBSI-SVol scores were higher than PBSI-CThi scores (Wilcoxon tests, HCP: $Z = 28.8$, $P = 4.10^{-182}$; CamCAN: $Z = 21.7$, $P = 8.10^{-105}$), indicating greater within-sample similarity for subcortical compared with cortical profiles.

PBSI Scores Differ Between Men and Women

Compared with men, women had higher PBSI-SVol scores (HCP: $Z = 3.21$, $P = 0.001$; CamCAN: $Z = 3.66$, $P = 4.10^{-4}$) and lower PBSI-CThi scores (HCP: $Z = 4.92$, $P = 9.10^{-7}$; CamCAN: $Z = 2.10$, $P = 0.036$) (Fig. 2*b*).

The PBSI Scores are Associated With Age

The relationship between age and PBSI-CThi was linear in the HCP sample while all other age-PBSI relationships were

quadratic, particularly in the CamCAN sample (R^2 > 9%, $P \leq 2.10^{-14}$) that includes data covering most of the adult lifespan (18–88 years) (Fig. 2c). To further characterize the association between the PBSI and age, we divided the samples into 3 age brackets representing early (range: 18–39 years), middle (40–59 years), and late (60–88 years) adulthood (Supplemental Table S2). The association between PBSI-CThi and age was not significant in early and middle adulthood and became negative and significant in late adulthood (CamCAN: Spearman's ρ = −0.41, $P = 3.10^{-12}$). The association between age and PBSI-SVol was positive in early (HCP: Spearman's ρ = 0.12, $P = 4.10^{-5}$; CamCAN: Spearman's $\rho = 0.22$, $P = 5.10^{-3}$) and middle adulthood (CamCAN: Spearman's ρ = 0.13, P = 0.06) but negative in late adulthood (CamCAN: Spearman's ρ = −0.28, $P = 4.10^{-6}$). The same pattern was identified when men and women were examined separately.

The degree of regional contribution to the PBSI in early, middle, and late adulthood appeared to be confirmed by known variation in age-associated regional changes in morphometry (Raz et al. 1997, 2004; Allen et al. 2005; Pfefferbaum et al. 2013). Specifically, across all age groups, the parahippocampal gyrus and the caudal anterior cingulate cortex bilaterally emerged as the most consistent contributors to the PBSI-CThi (Supplemental Fig. S1) while the contributions of the precentral gyrus and medial prefrontal regions increased with age. In contrast the contribution of the occipital regions decreased with age. The minimal contribution of the visual cortex to age-associated changes in PBSI-CThi is consistent previous studies which shown a weak correlation between visual cortex morphometry and age (Raz et al. 1997, 2004; Allen et al. 2005; Pfefferbaum et al. 2013) and are further supported by findings in nonhuman primates which suggest no age-related neuronal or volume loss in this region (Peters et al. 1997).

The PBSI Scores are Heritable

After covarying for age and sex, heritability estimates remained significant and of a similar magnitude for the PBSI-SVol (h^2=0.28, $P = 7.10^{-6}$) and the PBSI-CThi (h^2=0.29, $P = 3.10^{-8}$) scores (Supplemental Table S3).

The PBSI Scores are Robust to Variation in Regional Brain Measures

Bootstrap resampling and leave-one-out analyses confirmed that the PBSI scores in both samples were not dependent on the number of the contributing regional brain measures (Fig. 3). After each leave-one-out analysis, the recalculated scores remained within one standard deviation of the original values (Supplemental Table S4).

The PBSI-CThi Score is Associated With Fluid Intelligence

The effects of age (in the HCP sample), age^2 (in the CamCAN sample), and sex (both samples) were regressed out of the PBSI scores prior to estimating their association with the fluid and crystallized intelligence (details in Supplemental Table S1). No associations were found between both PBSIs and crystallized intelligence (r < 0.07, $P \geq 0.06$ uncorrected). By contrast, there was a significant bell-shaped association between the PBSI-CThi and fluid intelligence in both the HCP (r = 0.09, P = 0.044, after Bonferroni correction) and CamCAN (r = 0.13, P = 0.01, after Bonferroni correction) samples. Individuals with fluid intelligence scores that were 1.5 std below or above the mean had lower PBSI-CThi (Supplemental Fig. S2).

The PBSI-CThi Score is Negatively Associated With BMI in Men

The BMI was available in the HCP sample only (mean [std] = 26.5 (5.2)). In men, BMI was negatively associated with PBSI for cortical thickness (Spearman's ρ=−0.12, P = 0.008) and subcortical volume (Spearman's ρ=−0.09, P = 0.03) although the latter did not survive correction for multiple comparisons. None of these associations were significant in women (Spearman's ρ < −0.06, P > 0.1). The same pattern was identified after correcting for age.

The PBSI Scores are Reliable

The PBSI-CThi findings presented above were reproducible when the cortical parcellation was based on the Destrieux Atlas (Fischl et al. 2004). The ICC for scan–rescan reliability was markedly high for both PBSI-SVol (ICC = 0.92, 95% confidence interval [CI] = 0.85–0.95, $F_{44,44}$ = 12.90, $P = 2.10^{-14}$) and PBSI-CThi (ICC = 0.80, 95% CI = 0.63–0.89, $F_{44,44}$ = 5.0, $P = 2.10^{-7}$) based on data from 45 HCP participants scanned twice with an average interscan interval of 139 days (Supplemental Fig. S4). Finally, the PBSI-SVol and PBSI-CThi scores were reproducible with minimal variation when recalculated for random subsets of the HCP and CamCAN samples that included 10–90% of each sample participants in 10% increments (Supplemental Fig. S5).

Discussion

We introduce the PBSI, a novel metric that quantifies variation in brain structural profiles at the level of the individual person. The conceptual unit of analysis in the PBSI is the individual person's brain structural profile (either cortical or subcortical) which considers all relevant morphometric measures as features of a single vector. The PBSI approach therefore recognizes that each individual brain is a person-specific ensemble of interdependent regions. This is a fundamental departure from previous methods of assessing interindividual variation in which the units of analysis are discrete brain features. We demonstrated the foundational validity of this approach by affirming that the PBSI scores for subcortical volume (PBSI-SVol) and cortical thickness (PBSI-CThi) differ between men and women, are heritable, replicable and robust to variation in neuroimaging parameters (site, acquisition sequence, and analytical methods), sample composition, and regional brain morphometry. Additionally, individual variation in PBSI scores showed meaningful correlations with age, BMI and fluid intelligence.

The PBSI Scores Were Heritable

Thus far, all available heritability estimates concern discrete brain regions. Family-based heritability estimates range from 59% (pallidum) to 70% (hippocampus) for subcortical volumes and from 35% (entorhinal cortex) to 64% (postcental gyrus) for cortical thickness (McKay et al. 2014). A meta-analysis of twin studies (Blokland et al. 2012), provided heritability estimates for regional subcortical volumes (including the lateral ventricles) ranging from 53.2% to 58.5% for the right and left hippocampus to 78.4–81.6% for the left and right putamen. According to the same study, heritability estimates for regional cortical thickness ranged from 0.13% to 0.21% for the left and right insula to

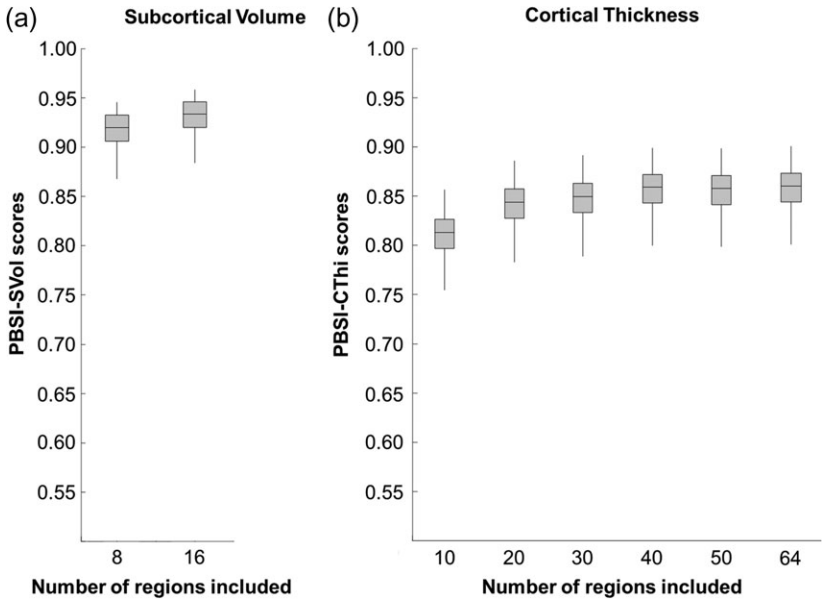

Figure 3. The person-based similarity index (PBSI) scores are robust to variation in number of regional brain measures. (*a*) PBSI for subcortical volume. (*b*) PBSI for cortical thickness. The boxplots shown are based on data from the Human Connectome Project; identical results were obtained in the Cambridge Center for Ageing and Neuroscience sample.

53.6–60.8% for the right and left superior frontal gyrus. Twin-based heritability estimates of cortical thickness in the HCP dataset range from nearly 0% for orbitofrontal regions to 64% for the left superior frontal gyrus, left superior parietal cortex and right postcentral gyrus (Strike et al. 2018). Collectively, the evidence points to large variations in the heritability of discrete brain structural features, the origins of which are not fully understood (Strike et al. 2018). In general, this variation has been found to be greater for cortical thickness than subcortical volume (Blokland et al. 2012; McKay et al. 2014). The fact that the PBSI-SVol and PBSI-CThi scores were also heritable suggests that genetic factors operate at the level of aggregate neuroanatomic variation, and not just at the level of specific brain regions. It should also be noted that while significant heritability estimates indicate that a particular trait is influenced by genetic factors in a specific population, they do not provide insights into the number or types of genes involved. Nevertheless our findings suggest the influence of "generalist genes," that is genes or genetic factors that influence neuroanatomic variation across multiple rather than specific features of anatomy. Similar arguments have been made about the genetic architecture of general intelligence versus more specific domains of cognition (Bearden and Glahn 2017).

PBSI Scores Differed Between Men and Women

Previous studies consistently show that men and women differ in terms of their mean brain regional volumes or cortical thickness (Ruigrok et al. 2014; Gur and Gur 2017). Few studies have examined sex differences in brain structural variation (Lange et al. 1997; Wierenga et al. 2017; Ritchie et al. 2018). Nonetheless it appears that across the lifespan the regional variance in subcortical volumes is lower in women than in men (Wierenga et al. 2017; Ritchie et al. 2018). The PBSI-SVol reflected this pattern as it was significantly higher in women than in men indicating greater similarity in subcortical profiles amongst women than amongst men. Regional variance in cortical thickness shows very subtle and largely nonsignificant sex differences (Wierenga et al. 2017; Ritchie et al. 2018). However, PBSI-CThi score was significantly lower in women than in men indicating less similarity in cortical profiles amongst women than amongst men. From these results we infer that the PBSI-CThi, which considers the entire cortical profile rather than individual regions, appears more sensitive to sex differences in cortical organization.

PBSI Scores and Age

To date all studies, both cross-sectional and longitudinal, that have examined the association between age and brain structure have used a variable-based approach. Collectively, these studies have shown that in healthy adults advancing age is associated with smaller subcortical volumes and thinner cortices (Fjell et al. 2010; Raz et al. 2010; Hedman et al. 2012; Dickie et al. 2013; Pfefferbaum et al. 2013; Storsve et al. 2014). Although the degree of age-related changes appears to vary significantly between brain regions and studies it is generally more pronounced after 60 years of age (Fjell et al. 2010; Raz et al. 2010; Hedman et al. 2012; Dickie et al. 2013; Storsve et al. 2014). It has also been shown that the variance in the morphometric measures across brain regions also increases with age (Resnick et al. 2003; Kruggel 2006; Farrell et al. 2009; Raz et al. 2010; Dickie et al. 2013; Pfefferbaum et al. 2013). The PBSI scores introduced here complement this field of research as we demonstrate that brain structural profiles become more dissimilar with age particularly after 60 years of age. The negative correlations between age and PBSI in late adulthood suggest that the cumulative effect of stochastic factors, biological or otherwise, over the lifespan may act to magnify individual variation both at variable and person-based measures of brain morphometry.

PBSI Scores and Fluid Intelligence

The relationship between brain structure and intelligence is complex and is likely to be influenced by diverse factors ranging from genetics to lifestyle choices and health maintenance decisions (Deary et al. 2010; Miller et al. 2016; Moser et al. 2018).

Variable-based analyses have found generally positive correlations between intelligence and cortical thickness, especially in the frontoparietal cortex and other multimodal association areas (Raz et al. 2008; Deary et al. 2010). Importantly, a recent study by Seidlitz et al. (2018) showed that higher fluid intelligence in healthy adults was correlated with the degree of similarity in their brain structural connectivity. These results resonate in part with our findings as the overall association of PBSI-CThi with fluid intelligence was positive. Of note, we found that the PBSI-CThi scores were lower in those with fluid intelligence scores that were either lower or higher than average. This indicates that even within the normal range of general intellectual ability, individuals at both extremes of the fluid intelligence distribution are more dissimilar in terms of their cortical thickness profiles compared with those with average fluid intelligence. We infer that the PBSI-CThi captures intelligence-related variation in cortical organization that is aligned with prior evidence of differences in cortical thickness and in the trajectories of cortical development between individuals with lower and higher intellectual ability (Shaw et al. 2006; Schnack et al. 2015; Navas-Sanchez et al. 2016).

The PBSI-CThi is Negatively Associated With BMI in Men

We focus on the BMI because it serves as a robust surrogate marker of cardiometabolic health; BMI is correlated with metabolic syndrome and insulin resistance (Esteghamati et al. 2008; Ryan et al. 2008) and is a reliable predictor of morbidity and mortality (Aune et al. 2016; Global et al. 2016). Higher BMI is also associated with brain structural variation (Miller et al. 2016; Moser et al. 2018) particularly in cortical thickness measures of prefrontal and posterior regions including the posterior cingulate, parietal, and occipital cortices (Willette and Kapogiannis 2015; Medic et al. 2016; Shaw et al. 2018). These findings are independent of sex (Willette and Kapogiannis 2015; Medic et al. 2016; Shaw et al. 2018). By contrast, we found that both PBSI-CThi and PBSI-SVol were negatively associated with BMI in men but not in women. Our findings suggest that the interaction between sex and BMI influences brain morphometric profiles, rather than individual variables. Of note, a recent study (Walhovd et al. 2014) noted that the inverse relationship between cortical thickness and BMI in men (but not women) was linked to higher serum cholesterol levels implicating sex difference in lipid metabolism that require further examination in future studies (Walhovd et al. 2014).

Methodological Considerations

We focused specifically on brain morphometry as assessed using structural MRI as it was critical to introduce this novel approach using imaging measures that are considered valid and reliable. However, a PBSI can be computed using data from any neuroimaging modality for multivariate phenotypes comprising more than 10 continuous variables. Computation of PBSI scores from different modalities would be an important addition to the work presented here. Although we examined the association of PBSI with age, sex, BMI, and fluid intelligence there are other behavioral and lifestyle variables that may be relevant that were not included here because of pragmatic considerations associated with availability. A particular strength of this study is the demonstration of test–retest reliability of the PBSI scores and the robustness of the PBSI approach to variation in neuroimaging parameters relating to acquisition and analysis, sample composition and regional brain morphometry.

Implications for Future Studies

The current results provide a novel approach for defining brain structural variation at the level of each individual person. Increased heterogeneity is traditionally invoked to explain the variable presentation of neuropsychiatric syndromes. The examination of heterogeneity in schizophrenia provides a typical example where the PBSI could prove useful. A large body of evidence has confirmed that brain morphometric alterations in this disorder involve multiple brain regions but with significant variability amongst patients (Gupta et al. 2015; van Erp et al. 2016, 2018). The PBSI is ideally suited to capture the brain imaging profile of each patient because it is computed using all the relevant regional values. The PBSI is a platform for identifying patients whose profile significantly differs from that of other patients thus enabling a detailed examination of the characteristics that may drive disease heterogeneity. The PBSI can also be used to quantify brain structural heterogeneity in a variety of clinical conditions and provide a new approach for linking brain structural variation to psychopathology, cognitive dysfunction, and cardiometabolic risk.

Supplementary Material

Supplementary material is available at *Cerebral Cortex* online.

Funding

National Institute of Mental Health (R01-MH104284-01A1; R01-MH116147 to S.F. and G.E.D.). National Institutes of Health (R01 MH080912 to D.C.G.). John D. and Catherine T. MacArthur Foundation, the Alfred P. Sloan Foundation, the Army Research Laboratory and the Army Research Office through contract numbers W911NF-10-2-0022 and W911NF-14-1-0679, the National Institute of Mental Health (R01-DC-009209-11), the National Institute of Child Health and Human Development (R01HD086888-01), the Office of Naval Research, and the National Science Foundation (BCS-1441502, BCS-1430087, NSF PHY-1554488) to D.S.B. Swiss National Science Foundation (P300PB_171584 to D.A.M.). HCP funding was provided by the National Institute of Dental and Craniofacial Research (NIDCR), the National Institute of Mental Health (NIMH), and the National Institute of Neurological Disorders and Stroke (NINDS). HCP data are disseminated by the Laboratory of NeuroImaging at the University of California, Los Angeles. The HCP data collection and sharing was provided by the MGH-USC HCP (NIH 1U54MH091657, http://www.humanconnectome.org/; Principal Investigators: Bruce Rosen, MD, PhD; Arthur W. Toga, PhD; Van J. Weeden, MD). The CamCAN data collection and was provided by the UK Biotechnology and Biological Sciences Research Council (Grant number BB/H008217/1), together with support from the UK Medical Research Council and University of Cambridge, UK. This work was supported in part through the computational resources and staff expertise provided by Scientific Computing at the Icahn School of Medicine at Mount Sinai.

Notes

Conflict of Interest: None declared.

References

Akshoomoff N, Beaumont JL, Bauer PJ, Dikmen SS, Gershon RC, Mungas D, Slotkin J, Tulsky D, Weintraub S, Zelazo PD, et al.

2013. VIII. NIH Toolbox Cognition Battery (CB): composite scores of crystallized, fluid, and overall cognition. Monogr Soc Res Child Dev. 78:119–132.

Allen JS, Bruss J, Brown CK, Damasio H. 2005. Normal neuroanatomical variation due to age: the major lobes and a parcellation of the temporal region. Neurobiol Aging. 26:1245–1260. discussion 1279-1282.

Almasy L, Blangero J. 1998. Multipoint quantitative-trait linkage analysis in general pedigrees. Am J Hum Genet. 62: 1198–1211.

Arslan S, Ktena SI, Makropoulos A, Robinson EC, Rueckert D, Parisot S. 2018. Human brain mapping: a systematic comparison of parcellation methods for the human cerebral cortex. Neuroimage. 170:5–30.

Aune D, Sen A, Prasad M, Norat T, Janszky I, Tonstad S, Romundstad P, Vatten LJ. 2016. BMI and all cause mortality: systematic review and non-linear dose-response meta-analysis of 230 cohort studies with 3.74 million deaths among 30.3 million participants. Br Med J. 353:i2156.

Bearden CE, Glahn DC. 2017. Cognitive genomics: searching for the genetic roots of neuropsychological functioning. Neuropsychology. 31:1003–1019.

Blangero J, Diego VP, Dyer TD, Almeida M, Peralta J, Kent JW Jr., Williams JT, Almasy L, Goring HH. 2013. A kernel of truth: statistical advances in polygenic variance component models for complex human pedigrees. Adv Genet. 81:1–31.

Blokland GA, de Zubicaray GI, McMahon KL, Wright MJ. 2012. Genetic and environmental influences on neuroimaging phenotypes: a meta-analytical perspective on twin imaging studies. Twin Res Hum Genet. 15:351–371.

Boedhoe PSW, Schmaal L, Abe Y, Alonso P, Ameis SH, Anticevic A, Arnold PD, Batistuzzo MC, Benedetti F, Beucke JC, et al, Group EOW. 2018. Cortical abnormalities associated with pediatric and adult obsessive-compulsive disorder: findings from the ENIGMA Obsessive-Compulsive Disorder Working Group. Am J Psychiatry. 175:453–462.

Cattell RB. 1971. Abilities: their structure, growth, and action. Boston: Houghton-Mifflin.

Deary IJ, Penke L, Johnson W. 2010. The neuroscience of human intelligence differences. Nat Rev Neurosci. 11:201–211.

Desikan RS, Segonne F, Fischl B, Quinn BT, Dickerson BC, Blacker D, Buckner RL, Dale AM, Maguire RP, Hyman BT, et al. 2006. An automated labeling system for subdividing the human cerebral cortex on MRI scans into gyral based regions of interest. Neuroimage. 31:968–980.

Dickie DA, Job DE, Gonzalez DR, Shenkin SD, Ahearn TS, Murray AD, Wardlaw JM. 2013. Variance in brain volume with advancing age: implications for defining the limits of normality. PLoS One. 8:e84093.

Esteghamati A, Khalilzadeh O, Anvari M, Ahadi MS, Abbasi M, Rashidi A. 2008. Metabolic syndrome and insulin resistance significantly correlate with body mass index. Arch Med Res. 39:803–808.

Farrell C, Chappell F, Armitage PA, Keston P, Maclullich A, Shenkin S, Wardlaw JM. 2009. Development and initial testing of normal reference MR images for the brain at ages 65-70 and 75-80 years. Eur Radiol. 19:177–183.

Fischl B, Liu A, Dale AM. 2001. Automated manifold surgery: constructing geometrically accurate and topologically correct models of the human cerebral cortex. IEEE Trans Med Imaging. 20:70–80.

Fischl B, Salat DH, Busa E, Albert M, Dieterich M, Haselgrove C, van der Kouwe A, Killiany R, Kennedy D, Klaveness S, et al. 2002. Whole brain segmentation: automated labeling of neuroanatomical structures in the human brain. Neuron. 33: 341–355.

Fischl B, Salat DH, van der Kouwe AJ, Makris N, Segonne F, Quinn BT, Dale AM. 2004. Sequence-independent segmentation of magnetic resonance images. Neuroimage. 23(Suppl 1): S69–S84.

Fjell AM, Walhovd KB, Westlye LT, Ostby Y, Tamnes CK, Jernigan TL, Gamst A, Dale AM. 2010. When does brain aging accelerate? Dangers of quadratic fits in cross-sectional studies. Neuroimage. 50:1376–1383.

Gelbard R, Goldman O, Spiegler I. 2007. Investigating diversity of clustering methods: an empirical comparison. Data Knowl Eng. 63:155–166.

Global BMIMC, Di Angelantonio E, Bhupathiraju Sh N, Wormser D, Gao P, Kaptoge S, Berrington de Gonzalez A, Cairns BJ, Huxley R, Jackson Ch L, Joshy G, et al. 2016. Body-mass index and all-cause mortality: individual-participant-data meta-analysis of 239 prospective studies in four continents. Lancet. 388:776–786.

Gupta CN, Calhoun VD, Rachakonda S, Chen J, Patel V, Liu J, Segall J, Franke B, Zwiers MP, Arias-Vasquez A, et al. 2015. Patterns of gray matter abnormalities in schizophrenia based on an international mega-analysis. Schizophr Bull. 41: 1133–1142.

Gur RC, Gur RE. 2017. Complementarity of sex differences in brain and behavior: from laterality to multimodal neuroimaging. J Neurosci Res. 95:189–199.

Heaton RK, Akshoomoff N, Tulsky D, Mungas D, Weintraub S, Dikmen S, Beaumont J, Casaletto KB, Conway K, Slotkin J, et al. 2014. Reliability and validity of composite scores from the NIH Toolbox Cognition Battery in adults. J Int Neuropsychol Soc. 20:588–598.

Hedman AM, van Haren NE, Schnack HG, Kahn RS, Hulshoff Pol HE. 2012. Human brain changes across the life span: a review of 56 longitudinal magnetic resonance imaging studies. Hum Brain Mapp. 33:1987–2002.

Hibar DP, Westlye LT, Doan NT, Jahanshad N, Cheung JW, Ching CRK, Versace A, Bilderbeck AC, Uhlmann A, Mwangi B, et al. 2018. Cortical abnormalities in bipolar disorder: an MRI analysis of 6503 individuals from the ENIGMA Bipolar Disorder Working Group. Mol Psychiatry. 23:932–942.

Holmes AJ, Hollinshead MO, Roffman JL, Smoller JW, Buckner RL. 2016. Individual differences in cognitive control circuit anatomy link sensation seeking, impulsivity, and substance use. J Neurosci. 36:4038–4049.

Horn JL, Cattell RB. 1966. Refinement and test of the theory of fluid and crystallized general intelligences. J Educ Psychol. 57:253–270.

Hulshoff Pol HE, Schnack HG, Posthuma D, Mandl RC, Baare WF, van Oel C, van Haren NE, Collins DL, Evans AC, Amunts K, et al. 2006. Genetic contributions to human brain morphology and intelligence. J Neurosci. 26:10235–10242.

Huttenlocher PR. 1990. Morphometric study of human cerebral cortex development. Neuropsychologia. 28:517–527.

Kanai R, Rees G. 2011. The structural basis of inter-individual differences in human behaviour and cognition. Nat Rev Neurosci. 12:231–242.

Karama S, Colom R, Johnson W, Deary IJ, Haier R, Waber DP, Lepage C, Ganjavi H, Jung R, Evans AC, Brain Development Cooperative G. 2011. Cortical thickness correlates of specific cognitive performance accounted for by the general factor of intelligence in healthy children aged 6 to 18. Neuroimage. 55:1443–1453.

Kievit RA, Davis SW, Griffiths J, Correia MM, Cam C, Henson RN. 2016. A watershed model of individual differences in fluid intelligence. Neuropsychologia. 91:186–198.

Koutsouleris N, Meisenzahl EM, Davatzikos C, Bottlender R, Frodl T, Scheuerecker J, Schmitt G, Zetzsche T, Decker P, Reiser M, et al. 2009. Use of neuroanatomical pattern classification to identify subjects in at-risk mental states of psychosis and predict disease transition. Arch Gen Psychiatry. 66:700–712.

Kruggel F. 2006. MRI-based volumetry of head compartments: normative values of healthy adults. Neuroimage. 30:1–11.

Lange N, Giedd JN, Castellanos FX, Vaituzis AC, Rapoport JL. 1997. Variability of human brain structure size: ages 4-20 years. Psychiatry Res. 74:1–12.

Lewitus E, Kelava I, Huttner WB. 2013. Conical expansion of the outer subventricular zone and the role of neocortical folding in evolution and development. Front Hum Neurosci. 7:424.

Lynch M, Walsh B. 1998. Genetics and analysis of quantitative traits. Sunderland: Sinauer Associates, Inc.

McKay DR, Knowles EE, Winkler AA, Sprooten E, Kochunov P, Olvera RL, Curran JE, Kent JW Jr., Carless MA, Goring HH, et al. 2014. Influence of age, sex and genetic factors on the human brain. Brain Imaging Behav. 8:143–152.

Medic N, Ziauddeen H, Ersche KD, Farooqi IS, Bullmore ET, Nathan PJ, Ronan L, Fletcher PC. 2016. Increased body mass index is associated with specific regional alterations in brain structure. Int J Obes. 40:1177–1182.

Miller KL, Alfaro-Almagro F, Bangerter NK, Thomas DL, Yacoub E, Xu J, Bartsch AJ, Jbabdi S, Sotiropoulos SN, Andersson JL, et al. 2016. Multimodal population brain imaging in the UK Biobank prospective epidemiological study. Nat Neurosci. 19:1523–1536.

Moser DA, Doucet GE, Lee WH, Rasgon A, Krinsky H, Leibu E, Ing A, Schumann G, Rasgon N, Frangou S. 2018. Multivariate associations among behavioral, clinical and multimodal imaging phenotypes in psychosis. JAMA Psychiatry. 75: 386–395.

Narr KL, Woods RP, Thompson PM, Szeszko P, Robinson D, Dimtcheva T, Gurbani M, Toga AW, Bilder RM. 2007. Relationships between IQ and regional cortical gray matter thickness in healthy adults. Cereb Cortex. 17:2163–2171.

Navas-Sanchez FJ, Carmona S, Aleman-Gomez Y, Sanchez-Gonzalez J, Guzman-de-Villoria J, Franco C, Robles O, Arango C, Desco M. 2016. Cortical morphometry in frontoparietal and default mode networks in math-gifted adolescents. Hum Brain Mapp. 37:1893–1902.

Panizzon MS, Fennema-Notestine C, Eyler LT, Jernigan TL, Prom-Wormley E, Neale M, Jacobson K, Lyons MJ, Grant MD, Franz CE, et al. 2009. Distinct genetic influences on cortical surface area and cortical thickness. Cereb Cortex. 19:2728–2735.

Peters A, Nigro NJ, McNally KJ. 1997. A further evaluation of the effect of age on striate cortex of the rhesus monkey. Neurobiol Aging. 18:29–36.

Pfefferbaum A, Rohlfing T, Rosenbloom MJ, Chu W, Colrain IM, Sullivan EV. 2013. Variation in longitudinal trajectories of regional brain volumes of healthy men and women (ages 10 to 85 years) measured with atlas-based parcellation of MRI. Neuroimage. 65:176–193.

Pintzka CW, Hansen TI, Evensmoen HR, Haberg AK. 2015. Marked effects of intracranial volume correction methods on sex differences in neuroanatomical structures: a HUNT MRI study. Front Neurosci. 9:238.

Rathore S, Habes M, Iftikhar MA, Shacklett A, Davatzikos C. 2017. A review on neuroimaging-based classification studies and associated feature extraction methods for Alzheimer's disease and its prodromal stages. Neuroimage. 155:530–548.

Raz N, Ghisletta P, Rodrigue KM, Kennedy KM, Lindenberger U. 2010. Trajectories of brain aging in middle-aged and older adults: regional and individual differences. Neuroimage. 51: 501–511.

Raz N, Gunning FM, Head D, Dupuis JH, McQuain J, Briggs SD, Loken WJ, Thornton AE, Acker JD. 1997. Selective aging of the human cerebral cortex observed in vivo: differential vulnerability of the prefrontal gray matter. Cereb Cortex. 7: 268–282.

Raz N, Gunning-Dixon F, Head D, Rodrigue KM, Williamson A, Acker JD. 2004. Aging, sexual dimorphism, and hemispheric asymmetry of the cerebral cortex: replicability of regional differences in volume. Neurobiol Aging. 25:377–396.

Raz N, Lindenberger U, Ghisletta P, Rodrigue KM, Kennedy KM, Acker JD. 2008. Neuroanatomical correlates of fluid intelligence in healthy adults and persons with vascular risk factors. Cereb Cortex. 18:718–726.

Raznahan A, Shaw P, Lalonde F, Stockman M, Wallace GL, Greenstein D, Clasen L, Gogtay N, Giedd JN. 2011. How does your cortex grow? J Neurosci. 31:7174–7177.

Resnick SM, Pham DL, Kraut MA, Zonderman AB, Davatzikos C. 2003. Longitudinal magnetic resonance imaging studies of older adults: a shrinking brain. J Neurosci. 23:3295–3301.

Ritchie SJ, Cox SR, Shen X, Lombardo MV, Reus LM, Alloza C, Harris MA, Alderson HL, Hunter S, Neilson E, et al. 2018. Sex differences in the adult human brain: evidence from 5216 UK Biobank participants. Cereb Cortex. 28:2959–2975.

Rocha-Rego V, Jogia J, Marquand AF, Mourao-Miranda J, Simmons A, Frangou S. 2014. Examination of the predictive value of structural magnetic resonance scans in bipolar disorder: a pattern classification approach. Psychol Med. 44: 519–532.

Ruigrok AN, Salimi-Khorshidi G, Lai MC, Baron-Cohen S, Lombardo MV, Tait RJ, Suckling J. 2014. A meta-analysis of sex differences in human brain structure. Neurosci Biobehav Rev. 39:34–50.

Ryan MC, Fenster Farin HM, Abbasi F, Reaven GM. 2008. Comparison of waist circumference versus body mass index in diagnosing metabolic syndrome and identifying apparently healthy subjects at increased risk of cardiovascular disease. Am J Cardiol. 102:40–46.

Schnack HG, van Haren NE, Brouwer RM, Evans A, Durston S, Boomsma DI, Kahn RS, Hulshoff Pol HE. 2015. Changes in thickness and surface area of the human cortex and their relationship with intelligence. Cereb Cortex. 25:1608–1617.

Segonne F, Dale AM, Busa E, Glessner M, Salat D, Hahn HK, Fischl B. 2004. A hybrid approach to the skull stripping problem in MRI. Neuroimage. 22:1060–1075.

Segonne F, Pacheco J, Fischl B. 2007. Geometrically accurate topology-correction of cortical surfaces using nonseparating loops. IEEE Trans Med Imaging. 26:518–529.

Seidlitz J, Vasa F, Shinn M, Romero-Garcia R, Whitaker KJ, Vertes PE, Wagstyl K, Kirkpatrick Reardon P, Clasen L, Liu S, et al. 2018. Morphometric similarity networks detect microscale cortical organization and predict inter-individual cognitive variation. Neuron. 97:231–247 e237.

Shafto MA, Tyler LK, Dixon M, Taylor JR, Rowe JB, Cusack R, Calder AJ, Marslen-Wilson WD, Duncan J, Dalgleish T, et al. 2014. The Cambridge Centre for Ageing and Neuroscience (Cam-CAN) study protocol: a cross-sectional, lifespan, multidisciplinary examination of healthy cognitive ageing. BMC Neurol. 14:204.

Shaw P, Greenstein D, Lerch J, Clasen L, Lenroot R, Gogtay N, Evans A, Rapoport J, Giedd J. 2006. Intellectual ability and cortical development in children and adolescents. Nature. 440:676–679.

Shaw ME, Sachdev PS, Abhayaratna W, Anstey KJ, Cherbuin N. 2018. Body mass index is associated with cortical thinning with different patterns in mid- and late-life. Int J Obes. 42: 455–461.

Sled JG, Zijdenbos AP, Evans AC. 1998. A nonparametric method for automatic correction of intensity nonuniformity in MRI data. IEEE Trans Med Imaging. 17:87–97.

Song C, Schwarzkopf DS, Rees G. 2013. Variability in visual cortex size reflects tradeoff between local orientation sensitivity and global orientation modulation. Nat Commun. 4:2201.

Storsve AB, Fjell AM, Tamnes CK, Westlye LT, Overbye K, Aasland HW, Walhovd KB. 2014. Differential longitudinal changes in cortical thickness, surface area and volume across the adult life span: regions of accelerating and decelerating change. J Neurosci. 34:8488–8498.

Strike LT, Hansell NK, Couvy-Duchesne B, Thompson PM, de Zubicaray GI, McMahon KL, Wright MJ. 2018. Genetic complexity of cortical structure: differences in genetic and environmental factors influencing cortical surface area and thickness. Cereb Cortex. doi: 10.1093/cercor/bhy002 [Epub ahead of print].

Taylor JR, Williams N, Cusack R, Auer T, Shafto MA, Dixon M, Tyler LK, Cam C, Henson RN. 2017. The Cambridge Centre for Ageing and Neuroscience (Cam-CAN) data repository: structural and functional MRI, MEG, and cognitive data from a cross-sectional adult lifespan sample. Neuroimage. 144:262–269.

Thompson PM, Hayashi KM, Dutton RA, Chiang MC, Leow AD, Sowell ER, De Zubicaray G, Becker JT, Lopez OL, Aizenstein HJ, et al. 2007. Tracking Alzheimer's disease. Ann N Y Acad Sci. 1097:183–214.

van Erp TG, Hibar DP, Rasmussen JM, Glahn DC, Pearlson GD, Andreassen OA, Agartz I, Westlye LT, Haukvik UK, Dale AM, et al. 2016. Subcortical brain volume abnormalities in 2028 individuals with schizophrenia and 2540 healthy controls via the ENIGMA consortium. Mol Psychiatry. 21:585.

Van Erp TG, Walton E, Hibar DP, Schmaal L, Jiang W, Glahn DC, Pearlson GD, Yao D, Fukunaga M, Hashimoto R, et al. 2018. Cortical brain abnormalities in 4474 individuals with schizophrenia and 5098 controls via the ENIGMA consortium. Biol Psychiatry. 84:644–654.

Van Essen DC, Smith SM, Barch DM, Behrens TE, Yacoub E, Ugurbil K, Consortium WU-MH. 2013. The WU-Minn Human Connectome Project: an overview. Neuroimage. 80:62–79.

van Rooij D, Anagnostou E, Arango C, Auzias G, Behrmann M, Busatto GF, Calderoni S, Daly E, Deruelle C, Di Martino A, et al. 2018. Cortical and subcortical brain morphometry differences between patients with autism spectrum disorder and healthy individuals across the lifespan: results from the ENIGMA ASD Working Group. Am J Psychiatry. 175:359–369.

von Eye A, Bogat GE. 2006. Person-oriented and variable-oriented research: concepts, results, and development. Merril-Palmer Q. 52:390–420.

Walhovd KB, Storsve AB, Westlye LT, Drevon CA, Fjell AM. 2014. Blood markers of fatty acids and vitamin D, cardiovascular measures, body mass index, and physical activity relate to longitudinal cortical thinning in normal aging. Neurobiol Aging. 35:1055–1064.

Wen W, Thalamuthu A, Mather KA, Zhu W, Jiang J, de Micheaux PL, Wright MJ, Ames D, Sachdev PS. 2016. Distinct genetic influences on cortical and subcortical brain structures. Sci Rep. 6:32760.

Whelan CD, Altmann A, Botia JA, Jahanshad N, Hibar DP, Absil J, Alhusaini S, Alvim MKM, Auvinen P, Bartolini E, et al. 2018. Structural brain abnormalities in the common epilepsies assessed in a worldwide ENIGMA study. Brain. 141:391–408.

Wierenga LM, Langen M, Oranje B, Durston S. 2014. Unique developmental trajectories of cortical thickness and surface area. Neuroimage. 87:120–126.

Wierenga LM, Sexton JA, Laake P, Giedd JN, Tamnes CK, Pediatric Imaging N, Genetics S. 2017. A key characteristic of sex differences in the developing brain: greater variability in brain structure of boys than girls. Cereb Cortex. 1–11.

Willette AA, Kapogiannis D. 2015. Does the brain shrink as the waist expands? Ageing Res Rev. 20:86–97.